The role of calcium and magnesium in the concrete tubes of the sandcastle worm

ChengJun Sun[1],*, Georg E. Fantner[2], Jonathan Adams[2], Paul K. Hansma[2] and J. Herbert Waite[1,3],*

[1]*Molecular, Cellular and Developmental Biology, [2]Physics Department and [3]Marine Science Institute and Chemistry and Biochemistry Department, University of California at Santa Barbara, Santa Barbara, CA 93106, USA*

*Authors for correspondence (e-mail: sun@lifesci.ucsb.edu; waite@lifesci.ucsb.edu)

Summary

Sandcastle worms *Phragmatopoma californica* build mound-like reefs by sticking together large numbers of sand grains with cement secreted from the building organ. The cement consists of protein plus substantial amounts of calcium and magnesium, which are not invested in any mineral form. This study examined the effect of calcium and magnesium depletion on the structural and mechanical properties of the cement. Divalent ion removal by chelating with EDTA led to a partial collapse of cement architecture and cement dislodgement from silica surfaces. Mechanical properties examined were sand grain pull-out force, tube resistance to compression and cement adhesive force. EDTA treatment reduced sand grain pull-out forces by 60% and tube compressive strength by 50% relative to controls. EDTA lowered both the maximal adhesive force and energy dissipation of cement by up to an order of magnitude. The adhesiveness of calcium- and magnesium-depleted cement could not be restored by re-exposure to the ions. The results suggest that divalent ions play a complex and multifunctional role in maintaining the structure and stickiness of *Phragmatopoma* cement.

Key words: *Phragmatopoma californica*, tube worm, protein cement, calcium, magnesium, biomechanics.

Introduction

The sandcastle worm *Phragmatopoma californica* (Fewkes) is a colonial intertidal reef builder (Hartman, 1944; Simmons et al., 2005). In collaboration with other worms, each sandcastle worm collects, inspects and cements wave-borne particles into the walls at the growing end of its home, a long concrete tube that is fused with the tubes of many other worms (Vovelle, 1965). The concretions made by a worm colony resemble honeycombed mounds that can be several meters in diameter (Vovelle, 1965; Jensen and Morse, 1988).

The particles that make up the walls of each tube are held together by droplets of cement that are sparingly dispensed by the building organ in the thorax of the worm. Each worm is thus continuously engaged in the manufacture of a composite material typically defined as a dispersion of stiff filler particles in a viscoelastic matrix (Wainwright et al., 1982). The cement, which serves as the matrix of the tube, was the subject of a recent extensive protein analysis. Three major protein families were identified (Waite et al., 1992; Zhao et al., 2005), two of which were basic and contain almost 10 mol% 3,4-dihydroxyphenylalanine (DOPA), whereas the third was acidic with very high levels of O-phosphoserine (Stewart et al., 2004). The proteins are deposited onto the sand surface as a colloidal emulsion rich in calcium (Ca) and magnesium (Mg) (Stewart et al., 2004) that sets within seconds. Cysteinyl-DOPA cross-links

are detectable in the cement and may reinforce the setting process (Zhao et al., 2005). The role of Ca^{2+} and Mg^{2+} ions in the cement is not understood, but recent atomic force microscopy (AFM) studies of bone suggest that Ca^{2+}-mediated interactions between bone mineral, collagen and phosphoproteins contribute significantly to the cohesiveness and fracture toughness of the bone structure (Fantner et al., 2005).

The sandcastle worm is not an important fouler of commercial surfaces, but presents useful features for studying wet adhesion. Its attachment strategy has much to teach about engineering durable adhesive bonds to wet mineral and metal surfaces, a feat that eludes most synthetic polymers (Brockmann, 1983). Indeed, environmental moisture is the leading cause of adhesive failure in manufactured products, including silica-filled composites (Comyn, 1982).

The aim of the present study was to explore the contribution of the divalent ions to the mechanical performance of the *Phragmatopoma californica* cement. Three hypotheses were tested: (1) Ca and Mg contribute to the compressive strength of worm tubes, (2) Ca and Mg provide cemented sand grains with resistance to pull-out forces, and (3) Ca and Mg are crucial for adhesion of the cement. Our results indicate that divalent ions Ca^{2+} and Mg^{2+} play crucial roles in the structural integrity and cohesive strength of the *Phragmatopoma* cement.

Materials and methods

Tube production

The protocol for inducing new tube production has been detailed previously (Stewart et al., 2004). Briefly, colonies of *P. californica* collected from the intertidal zone near Campus Point, Santa Barbara, CA, USA were transferred to shallow laboratory tanks circulated with seawater at ~12°C. Single worms residing in only 1–2 cm of their original tube length were spaced out on a bed of clean sand or glass beads. Commercial sand (grain size range 400–600 μm) was obtained from Sigma and placed in a large Petri dish maintained under flowing filtered and aerated seawater. The worms extended the anterior tube ends with the available clean sand. A batch of the newly built tube increments was harvested regularly and washed with either filtered seawater or deionized water followed by five washes with Milli-Q water. A batch here refers to all of the tubes made under the same condition by a newly collected cohort of worms during a given period in captivity. Depending on the experiment, the tubes were then incubated in different treatment solutions.

Special conditions were required for construction of tubes used for pull-out tests. The worms were placed on a single layer of sand or glass beads in a 13-cm diameter Petri dish, with the bottom of the dish covered with small coverslips (18 mm×18 mm, 0.13–0.16 mm thick) affixed to the Petri dish with double-sided tape. Newly built portions of the tubes on coverslips usually resembled tunnels because the worm used the coverslip surface as one facet of the tube. The newly built tubes were harvested with the attached coverslip and subjected to further treatment and mechanical analysis.

EDTA treatment

Following eviction of the resident worm, freshly collected and washed tube increments including the coverslip were incubated in 250 mmol l^{-1} EDTA (pH 8.0) at room temperature under very gentle shaking for 24 h. For the pull-out test, coverslip-associated tubes were mounted directly onto the miniature force gauge and then tested. For morphological examination, the EDTA-treated sand tubes were broken apart and residual salts were removed with deionized and Milli-Q water washes. Some of the tubes were also broken apart prior to EDTA treatment to probe the effect of EDTA on detached cement. Washed sand grains were then freeze-dried and mounted on scanning electron microscopy (SEM) posts for imaging (refer to the later SEM imaging section for details). *log* stability constants for the formation of EDTA–Ca and EDTA–Mg complexes are 10.7 and 8.7, respectively (Dawson et al., 1986).

Pull-out force test

The pull-out or detachment force of sand grains was measured using the worm tubes attached to coverslips, the latter providing an adequate amount of flat surface to be secured to the spring arm by a pair of magnets. The pull-out test system is based on a simple spring gauge, as shown in Fig. 1. The spring was a flat strip of type 302 steel (width 10 mm and thickness 0.127 mm), which was fixed in a vise at one end and bent 90° at the other, 56 mm from the vise mount. The bent overhang was 18 mm long, which was adequate to enable a pair of magnets to secure a coverslip with attached tube. Sand grains were pulled from the end of a worm tube one at a time with fine-tipped forceps (Dumont type #3) in a trajectory perpendicular to the long axis of the spring and at a pulling speed of approximately 0.5 mm s^{-1} based on calculations from video-recordings. Pull-outs were monitored under a light microscope. Spring deflection, which was measured by ruler with an accuracy of 0.5 mm, gauged the pull-out force and was converted to Newtons by comparison with a standard calibration curve determined by using a microbalance (Mettler Toledo, 0.1 mg readability). The spring was calibrated by measuring deflections for a range of known metric loads. The force at each deflection was calculated according to force=mass×acceleration of gravity.

A total of 81 and 134 sand grains were pulled from a batch of approximately 10 EDTA-treated and untreated tubes,
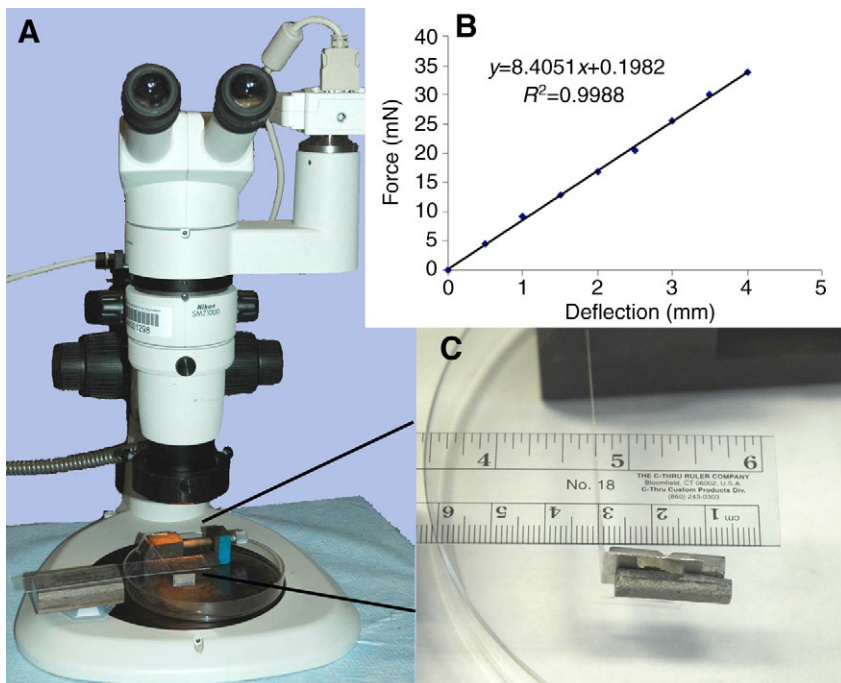

Fig. 1. Set-up of miniature force gauge (A) and force calibration curve (B). Force was measured by the deflection of the stainless steel arm. The worm tube on a coverslip was secured to the spring arm by being sandwiched between a pair of magnets, as shown in the close-up picture of the deflection measurement set-up (C). Pull-out tests were viewed at a magnification of 40 using a binocular light microscope.

In figure B:
$$y=8.4051x+0.1982$$
$$R^2=0.9988$$

respectively. The sample number for EDTA treatment is lower only because many of the tubes did not survive the EDTA treatment. The tubes we used came from different worms. However, each tube from the same worm was divided into at least two sections (depending on how many pieces of the coverslips the tube resided on) and were treated with seawater and EDTA, respectively, to minimize sample variation. The Kolmogorov–Smirnov test was used for statistics.

Mechanical compression

Compressive loading of tubes was performed with a mechanical tester (Bionix 200; MTS Systems, Cary, NC, USA) equipped with a 10-N load cell set at a cross-head speed of $1\ mm\ min^{-1}$. Worm tubes were placed on a flat stainless-steel mount and secured at both ends by tape. Force and deformation were recorded while the end of a motor-driven steel plate with a $2.5\ mm \times 40\ mm$ cross-section was pushed at right angles against the long axis of the tube. All samples were wet-tested (capillarity was adequate to completely wet the tube) with the appropriate treatment buffer. Each tube was tested to compressive failure, which was defined as the point at which visible structural collapse occurred. A batch of 18 tubes was tested. Each worm tube was divided in two, one half subjected to EDTA treatment and the other half subjected to seawater treatment. Change in the peak load was expressed as the $N_{EDTA}/N_{seawater}$. In order to look into the effect of Milli-Q water wash, we also tested another 16 tubes with half of each tube rinsed and tested in Milli-Q water and the other half of each tube rinsed and tested in seawater. Results were also expressed as $N_{Milli-Q\ water}/N_{seawater}$ for inter-sample comparison.

SEM imaging and energy dispersive spectrometry (EDS)

For SEM imaging, tubes built from glass beads were preferred on account of the uniformity of the beads and cement deposits. Following each treatment, glass beads were extensively rinsed with Milli-Q water to eliminate residual salt, followed by freeze-drying and mounting on SEM posts. The samples were sputter-coated with gold for 60 s for imaging and 15 s for *in situ* elemental analysis using a Denton Vacuum DESK II coater (45 mA, 6.666 Pa) (Moorestown, NJ, USA), and examined with a Tescan Vega TS 5130MM thermionic emission scanning electron microscope equipped with an IXRF Systems energy dispersive spectrometer (Tescan, Houston, TX, USA). Sample pore size and trabecular (distance between the pores) thickness were measured by using the measurement function that comes with the Tescan software.

AFM test on cement in seawater and EDTA

To measure the adhesion of *Phragmatopoma* cement under cyclic stress–strain conditions, AFM experiments were performed using cement deposits or 'glue prints' on coverslips. Because of the nonhomogeneity of the cement patches, a 50 μm glass bead was glued to the end of an AFM cantilever (CSC21; Mikromash USA, Wilsonville, OR, USA) using 2-ton epoxy (Devcon, Danvers, MA, USA). The beaded cantilever was positioned over a cement patch using the OMV optical microscopy system of a Multimode Picoforce system (Veeco, Santa Barbara, CA, USA). The bead tip was held on the surface with a force of 10 nN for 3 s for each pull. Pulling experiments were performed at a rate of 0.33 Hz. Sufficient protein adhesion to the bead tip during a 'pick-up' is provided by multiple noncovalent interactions (Rief et al., 1997). Pulling curves were first performed in seawater (several-hundred pulls), after which the sample chamber was flushed with EDTA ($500\ mmol\ l^{-1}$, pH 8.0) in which another several-hundred pulls were performed at the same position. Water-rinse effect after seawater was also investigated. The pulling curves were analyzed for energy dissipation, maximum adhesion force and pulling length using custom software written in LabView 7.1 (National Instruments, Austin, TX, USA). Statistical analysis reflecting the change in adhesion from seawater to EDTA was performed in Origin 7 (OriginLab, Northhampton, MA, USA) using an independent Student's *t*-test at a significance level of 0.05. Because of the nature of the testing, only one out of many glue spots on each coverslip could be tested with a set of experiments. In all, five different cement prints from five different worms were tested and analyzed.

Results

SEM imaging on the morphological effect of EDTA on the cement

The cement deposited by the sandcastle worm onto sand grains is disc-shaped with a skin-covered porous structure (Fig. 2A-D). Cement porosity was explored following cohesive and adhesive failure. In cohesive failure, breakage occurred within the cement, whereas in adhesive failure the cement peeled away from the sand particle. The pores exhibited in broken cement (Fig. 2C,D) had diameters that averaged approximately 695 nm (s.d.=496 nm, N=1951 from two images) and ranged from 100 nm to 4 μm. These data are consistent with an earlier study (Stewart et al., 2004). The trabecular structure of each pore consisted of a thin pore wall (30–50 nm thickness) and a connecting matrix approximately 166 nm thick (range 42–599 nm with an s.d. of 60 nm, N=1724 from three images). Adhesive failure revealed a deeply dimpled interfacial 'footprint'. Curiously, although a thin skin covered both the exposed and interfacial portions of the cement, only the skin of the interfacial portion appeared to be sufficiently compliant to dimple.

The effect of EDTA on tube cement morphology depended largely on the integrity of the skin. EDTA treatment of cement with intact skin often resulted in cement dislodgement from one or both surfaces (Fig. 2E). Examination of cement fractured after EDTA treatment revealed an internal porous structure but with greater distortion, e.g. stretched trabeculae and ovate pores (Fig. 2H). When the cement was fractured prior to EDTA treatment, the porous structure collapsed completely, revealing many stretched or bent trabeculae (Fig. 2F,G). Trabecular structure analysis revealed that the mean matrix thickness in
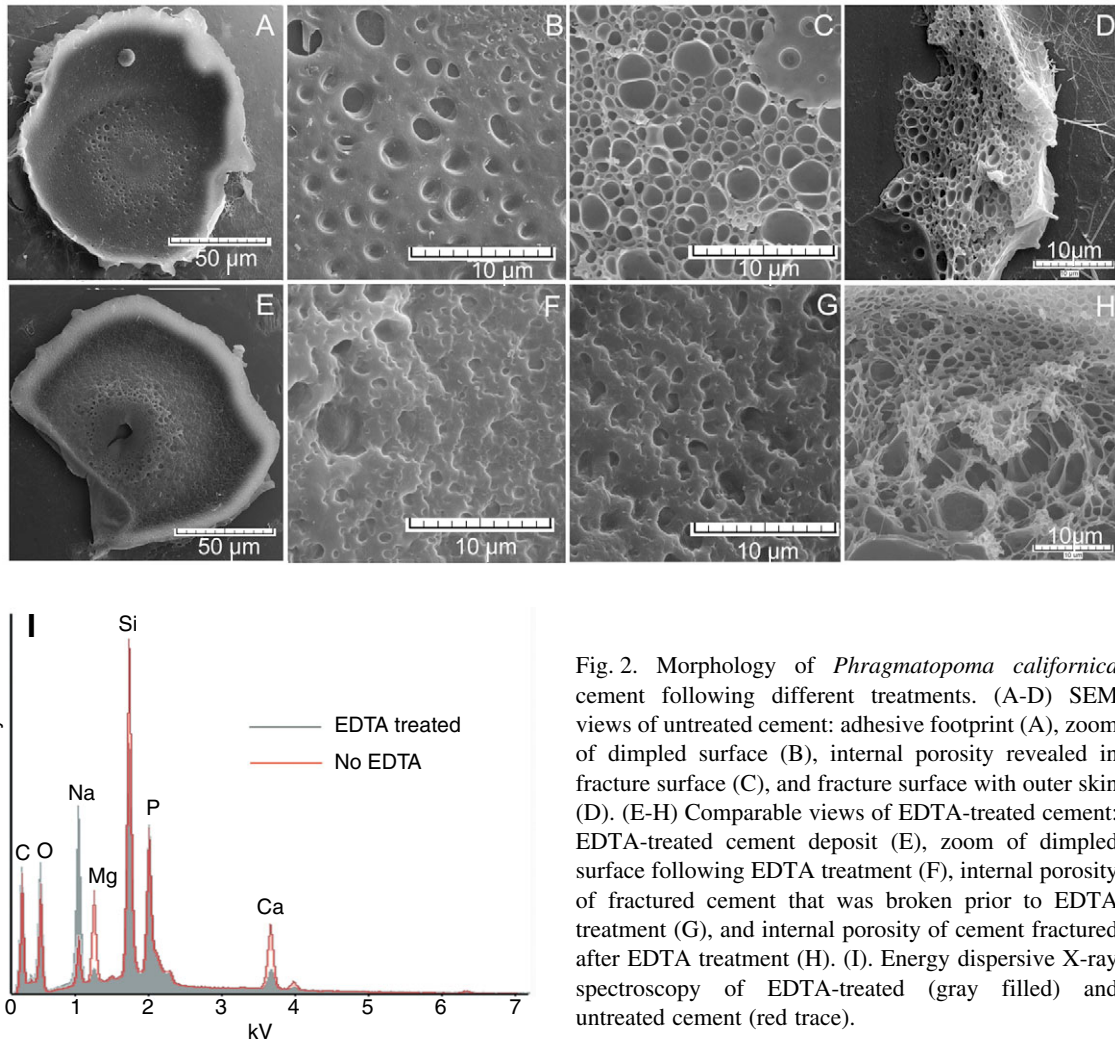
Fig. 2. Morphology of *Phragmatopoma californica* cement following different treatments. (A-D) SEM views of untreated cement: adhesive footprint (A), zoom of dimpled surface (B), internal porosity revealed in fracture surface (C), and fracture surface with outer skin (D). (E-H) Comparable views of EDTA-treated cement: EDTA-treated cement deposit (E), zoom of dimpled surface following EDTA treatment (F), internal porosity of fractured cement that was broken prior to EDTA treatment (G), and internal porosity of cement fractured after EDTA treatment (H). (I). Energy dispersive X-ray spectroscopy of EDTA-treated (gray filled) and untreated cement (red trace).

the trabeculae was approximately 505 nm (range 111 nm–1.39 µm with an s.d. of 218 nm, N=526 from two images), which is significantly higher than that from an untreated sample. Perhaps the complete collapse of several adjacent pores may be leading to stacks of fused trabeculae. The greater retention of structure in cement with intact skins suggests that the skins might retard diffusion of EDTA. The only detectable EDTA-induced chemical change in the cement as mapped by EDS was the depletion of Ca and Mg (Fig. 2I), which is consistent with earlier studies (Stewart et al., 2004).

Binding force test results on normal and EDTA-treated tube

Because of the technical difficulty of testing singly bonded pairs of sand grains, a miniature force gauge was designed to measure the pull-out strength per sand grain in tubes made by worms maintained in laboratory tanks. For the untreated tubes tested in seawater, approximately 70% of the sand grains exhibited a pull-out force greater than 21 mN (Fig. 3). With regard to the EDTA-treated tubes, over 80% of the sand grains had a pull-out force of 9 mN or less (Fig. 3A). It must be emphasized that no pull-out measurements could be made for many of the sand grains (~40% of total) because, as noted

earlier, cement contacts were frequently dislodged by EDTA treatment. On average, the untreated sand grains required approximately three times more pull-out force than the surviving EDTA-treated ones. The Kolmogorov–Smirnov test showed this difference between EDTA-treated and untreated grains to be highly significant (Fig. 3B).

Compression tests on untreated and EDTA-treated tubes

Fig. 4 shows the compressive failure for a laboratory-grown tube that occurred at approximately 0.47 N compared with 0.11 N for the EDTA-treated counterparts produced by the same worm. The difference between the two is approximately two- to threefold. The magnitude of peak force varied with tubes from different worms and tubes from the same worm during different time periods. In order to compare results from the same batch of samples, we used $N_{treatment}/N_{without\ treatment}$ to represent the change. Our result showed that $N_{EDTA}/N_{seawater}$ was approximately 0.49 (table in Fig. 4). We also compared samples in seawater with those rinsed and washed with Milli-Q water. Results showed that $N_{milli-Q\ water}/N_{seawater}$=0.91±0.25 (Fig. 4). EDTA treatment dramatically decreased the peak load, whereas the Milli-Q water wash did not seem to
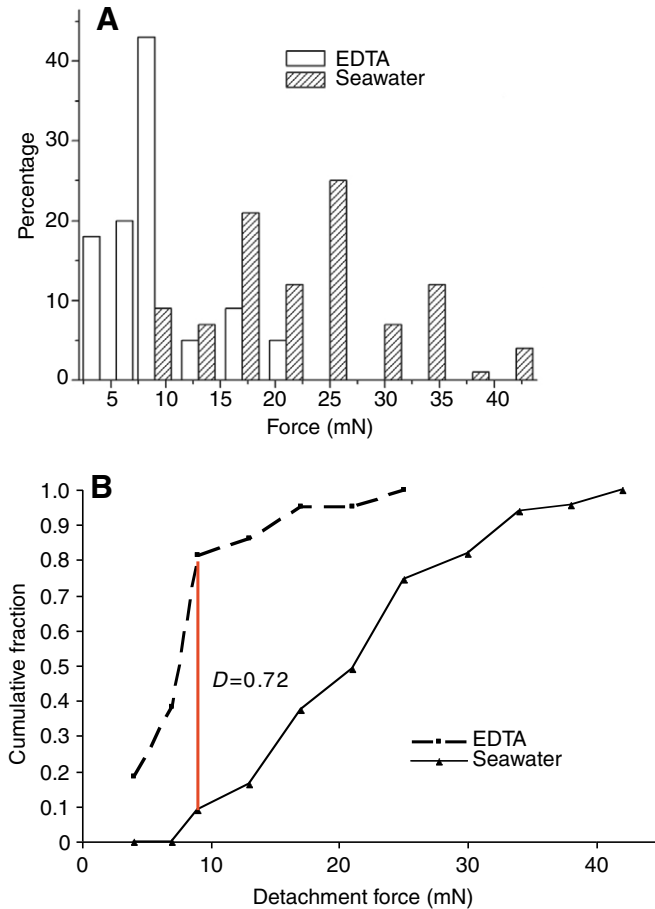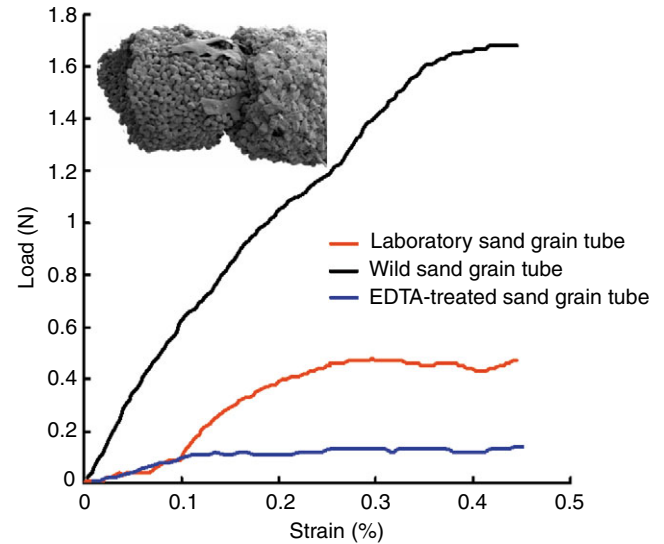
Fig. 3. (A) Distribution of pull-out force per sand grain as tested on EDTA-treated (*N*=81) and untreated sand (silica) tubes in seawater (*N*=134), and (B) the cumulative fraction plot of EDTA- and seawater-treated tubes showing that the difference between the two treatments was statistically significant.

Fig. 4. Behavior of 'wild', untreated laboratory-grown tubes and EDTA-treated laboratory-grown tubes subjected to compression. Inset shows SEM image of a piece of hybrid tube showing the original wild tube (right) extended with commercial acid-washed sand (left) by the resident worm. The table shows statistical results of the peak load ratio between different treatments.

significantly weaken the tube. It is noteworthy that sand tubes collected from the wild and subjected to compression exhibited peak loads as high as 1.68 N (between 1.25–2.28 N for a typical tube having dimensions of 3–3.5 mm outer diameter and 2 mm inner diameter), more than four times that of the untreated laboratory-grown tubes. The most obvious differences between the wild and laboratory-grown tubes were tube wall thickness and grain size (Fig. 4 inset). Wild tube walls tended to be much thicker (7–10 equivalent sand grain diameters *versus* 3–4 sand grains for laboratory-grown tubes) and were constructed from a wider range of grain sizes, shapes and materials. All these factors contributed to the construction of gap-free tube walls.

AFM test results of EDTA-treated cement (with and without Ca and Mg)

AFM was used to investigate the nanoscale adhesive properties of the tube cement. A cantilever with an attached glass bead (see Fig. 5A) was pressed onto the edge of a cement deposit on a coverslip to prevent picking up too much

cement. During cantilever retraction, adhesion resulted in force–distance pulling curves like those shown in Fig. 5B, which are representative for pulls in seawater and EDTA, respectively. The approach-retraction cycle was repeated 500 times at the same spot in seawater and then another 500 times after flushing with EDTA. For each trial, the averages of total pulling length, maximum force and total energy dissipation were calculated (one trial shown in Fig. 5C). Because of the inhomogeneous nature of the cement deposits, the absolute values of the pulls varied considerably. These variations could have been caused by the heterogeneity in the cement deposits, by a slight drift in the pulling position or by distortion of the cement deposit by the cantilever. To make comparisons between samples easier, the absolute values were normalized to the seawater value for each trial. For all five trials, all of the changes in measured adhesion parameters from seawater to EDTA were statistically significant at *P*=0.05. Fig. 5D shows the time dependence of the adhesion for the trial shown in Fig. 5C, with each point representing one pull. The approach-retraction cycle was repeated 500 times at the same spot in seawater and then another 500 times after flushing with EDTA. To ensure that the reduction in adhesion by EDTA was not just an effect from rinsing, we also flushed the sample chamber with seawater after the first 250 pulls and found no significant effect (*P*=0.05). In addition, tests in Milli-Q water after seawater did not show significant difference between the two.
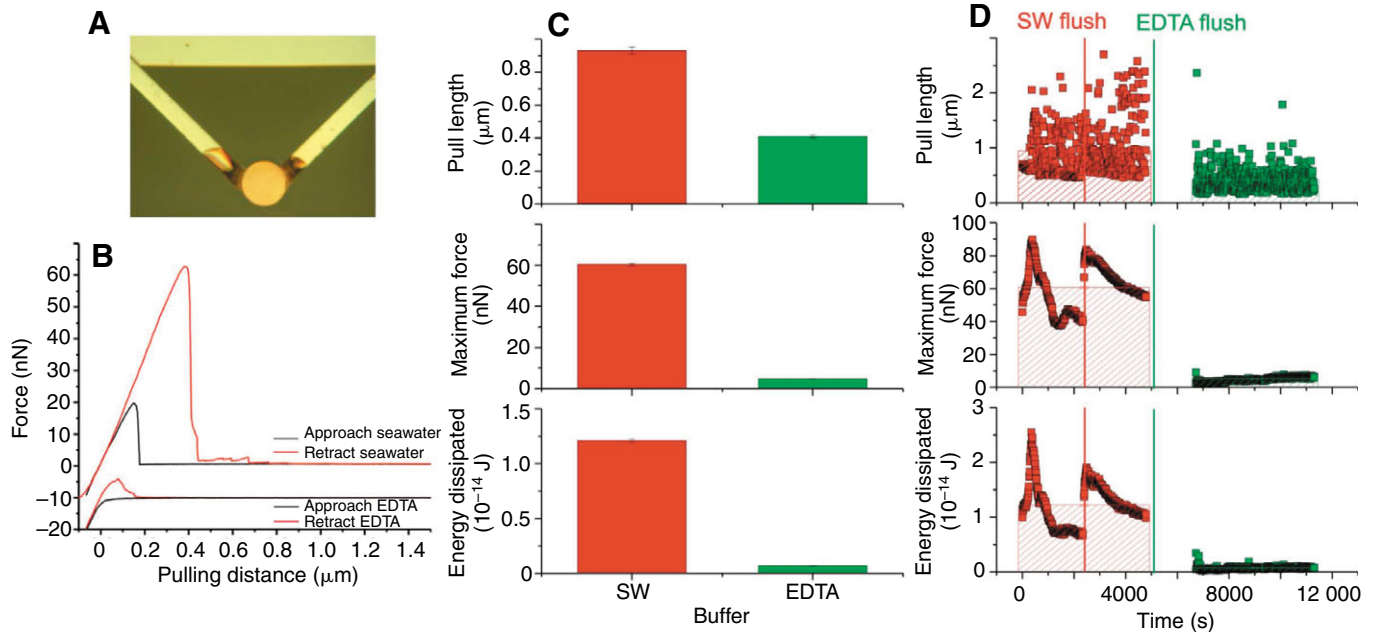
Fig. 5. Atomic force microscopy (AFM) of untreated and EDTA-treated cement deposits on glass coverslips. Each approach-retract curve represents an adhesive test performed on a single cement spot. An AFM cantilever with a glass bead attached to the end (A) is brought into contact with the edge of the cement and pressed down with 10 nN for 3 s. The EDTA curves are offset by −10 nN for clarity. With cantilever retraction, an adhesion force is measured (B) (curves are offset by 10 nN for better visibility). After 500 pulls at the same spot, the chamber was flushed with EDTA and 500 pulls were recorded at the initial spot. The pulling length, maximum force and energy dissipation were calculated for each trial (500 pulls for each condition on one sample). One trial is shown in (C); error bars represent s.d.; SW, seawater. (D) The repeatability and the time dependence of the adhesion for the trial shown in C, with each square representing one pull.

The adhesion loss following EDTA treatment was not recoverable by extensive flushing with seawater (data not shown).

Discussion

Sandcastle worm tubes represent an intriguing concretion of two components – a plethora of mostly abiotic particulate matter and an organic cement that sparingly binds it together. The cement of *Phragmatopoma* and related sabellariids was previously shown to be rich in Ca and Mg (Gruet et al., 1987). At one time the metals were thought to be present as minerals, possibly calcium/magnesium phosphate (Gruet et al., 1987), but evidence for this has never materialized (Stewart et al., 2004). Indeed, the phosphate appears to be entirely associated with the phosphorylated Pc-3 proteins in the cement (Zhao et al., 2005). The aim of this research was to assess the contribution of Ca/Mg to the mechanical properties of the worm tubes. This was done by measuring the effects of divalent ion removal using EDTA, a divalent ion chelator. EDTA is not specific for Ca/Mg, but chelates a variety of ions, including some such as Cu^{2+} with extremely high affinity (log K_s=18.8). Compositional analysis of the cement by EDS before and after EDTA treatment, however, showed convincingly that Ca/Mg removal was the only detectable chemical effect of the treatment (Stewart et al., 2004) (Fig. 2i).

The mechanical effects of Ca/Mg removal were explored at several levels ranging from the macro- to nanoscale. The compressive strengths of whole tubes made under laboratory conditions with commercial sand exhibited only a quarter of the strength of tubes collected from the wild, but were at least twice as strong as the EDTA-treated laboratory tubes. The wild-type tubes were not subjected to EDTA treatment because they included a high proportion of calcareous particles, which would have been dissolved by EDTA. By contrast, the laboratory-made tubes were built using only silica-based sand, which could confidently be assumed to be inert towards EDTA. The superior strength of wild-type tubes should be subjected to closer scrutiny in future analyses. At present we attribute the better wild-type performance to three factors: use of a wider range of particle sizes, more irregular particles and particle packing with fewer (if any) gaps. Additional factors are of course also possible.

To investigate microscale mechanics, the pull-out force of sand grains from laboratory-made tubes was measured. Sand grains from the untreated tubes required two to three times more pull-out force than the EDTA-treated ones. The magnitude of this effect was somewhat different than that in the compression tests, but not unexpected because the two tests were measuring different properties. In pull-outs, the mechanical properties most directly tested were the tensile and shear strengths of the cement and thus would be closely linked to the structural integrity of the cement itself. EDTA treatment caused the rigid, porous cement structure to collapse (Fig. 2E-

H). Judging by the number of stretched trabeculae and distorted pore shapes, Ca/Mg depletion appeared to soften the cement. It is possible that EDTA removed components in addition to Ca/Mg, but this remains to be determined.

Nanomechanical analysis of cement deposits was performed with a modified AFM cantilever. EDTA treatment greatly diminished both the maximum observed adhesive force and energy dissipation of cement; extensibility as approximated by pull-out length also decreased by approximately 50% but there was much variability. For the untreated cement tested in seawater, the approach-retract cycles were largely reversible. The energy dissipation, maximum adhesion force and the pulling length were not significantly diminished after 500 AFM pulls in seawater. This suggests that the cement depends on noncovalent interactions that can reform with re-established contact and which would enable considerable 'rehealing' following moderate deformation. After EDTA treatment, however, this 'self-healing' ability was lost even after reintroduction of Ca/Mg.

The emerging picture reveals a cement that is fairly robust and with a striking dependence on Ca/Mg. An approximate adhesive strength can be calculated from the mean sand grain pull-out force of 25 mN. Given that each sand grain or glass bead is typically held in place by four to five spot 'welds' of the cement, approximately 5–6 mN would be required to break each spot. Taking 6 mN as the breaking force for one spot with a diameter of 150 μm gives an estimated adhesive strength of 350 kPa. This is consistent with other marine adhesives such as mussel byssus, which on glass exhibited an adhesive strength of 320 kPa in the winter and 750 kPa in summer (Young and Crisp, 1982). Two caveats, however, are worth mentioning for this comparison: (1) our pull-out tests involved a mixed mode of loading (tensile and shear) that may not be comparable to the mechanical tests used in other studies; and (2) given the mechanical superiority of field specimens, it is possible that laboratory conditions (including the building material, silica sand) are not optimal for cement maturation. In view of these considerations, our estimate of strength should be treated as a minimum.

The dependence of cement performance on Ca/Mg is intriguing because it superficially resembles Ca-dependent cell–cell adhesion. Adhesion between cells is mediated by cadherins, which are modular proteins extending out from the cell surface. Although the interactions between cadherins from different cells are not directly Ca-mediated, cadherin conformation and rigidity are (Leckband and Sivasankar, 2000; Nagar et al., 1996; Prakasam et al., 2006); thus, with Ca depletion, cadherins unravel, and the three-dimensional conformation-dependent adhesive contact surfaces lose their identity.

Is a similar mechanistic understanding of adhesion in *Phragmatopoma* cement possible at this point? Practical adhesion is governed by two overriding factors – the strength and number of interfacial interactions between the cement and a surface and the cohesive strength or 'cure' of the cement (Fig. 6). Is the Ca/Mg dependence of cement a reflection of
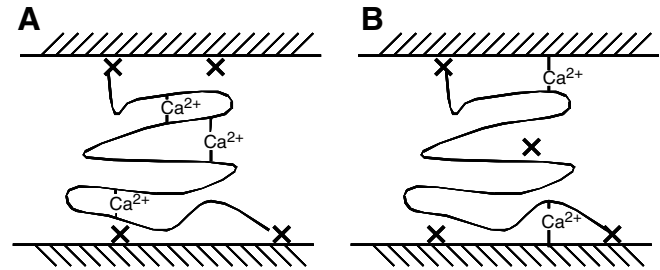

Fig. 6. Models of the interfacial and cohesive paradigms of Ca/Mg involvement in the adhesion of *Phragmatopoma californica* cement. (A) Ca/Mg provides inter- and intramolecular bridges for Pc-3 proteins within the cement. (B) Ca/Mg provides interfacial bridges between cement proteins and anionic surface groups. The cross symbols indicate other types of interactions.

interfacial activity or curing? Wholesale dislodgement of cement discs from sand and glass beads following EDTA treatment suggests interfacial involvement, as does the decreased adhesive force in AFM. The repertory of building materials for sabellariids, however, is larger than silica so the proposed model (Fig. 6B) may not apply to all surfaces. Indeed, silica surfaces are negatively charged at seawater pH (Neihof and Loeb, 1972), providing a perfect setting for ion bridging by Ca and Mg. However, the structural collapse in the cement, evidence of increased stretching and bending in the trabecular network, as well as the lower slopes in the compression plots (Fig. 4) are more suggestive of a structural cohesive role for Ca/Mg as proposed for Ca in the frustule of diatoms (Kröger et al., 1994) and in the PEVK region of titin (Kellermayer and Bustamante, 1997; Labeit et al., 2003). At this stage, given the narrow scope of this study, we can conclude only that the role of Ca/Mg in *Phragmatopoma* cement is crucial and multifunctional.

The defining significance of Ca/Mg in the performance of *Phragmatopoma* cement seems to mystify the role of DOPA, an amino acid commonly present in marine adhesives (Waite et al., 2005). Indeed, two of the cement precursors, Pc-1 and Pc-2, each contain almost 10 mol% DOPA (Waite et al., 1992). The detection of cysteinyl-DOPA cross-links in the cement suggests DOPA plays a role in the curing of the structure (Zhao et al., 2005). However, such covalent cross-links would not have been labile to EDTA treatment. In addition, the interfacial coordination complexes formed between peptidyl-DOPA and surface oxides (Lee et al., 2006) are considerably more stable than the corresponding ones with EDTA. Additional adhesive mechanisms and interactions will undoubtedly emerge as particulates other than silica are tested under conditions more akin to those occurring in the wild.

References

Brockmann, W. (1983). Durability of metal polymer bonds. In *Adhesion Aspects of Polymer Coatings* (ed. K. L. Mittal), pp. 265-280. New York: Plenum.

Comyn, J. (1981). The relationship between joint durability and water diffusion. In *Developments in Adhesives-2* (ed. A. J. Kinloch), pp. 279-313. Barking: Applied Science.

Dawson, R. M., Elliott, D. C., Elliott, W. H. and Jones, K. M. (1986). *Data for Biochemical Research*. Oxford, New York: Oxford University Press.

Fantner, G. E., Hassenkam, T., Kindt, J. H., Weaver, J. C., Birkedal, H., Pechenik, L., Cutroni, J. A., Cidade, G. A. G., Stucky, G. D. and Morse, D. E. (2005). Sacrificial bonds and hidden length dissipate energy as mineralized fibrils separate during bone fracture. *Nat. Mat.* **4**, 612-616.

Gruet, Y., Vovelle, J. and Grasset, M. (1987). Biomineral components of tube cement of *Sabellaria alveolata* (L), (Annelida Polychaeta). *Can. J. Zool.* **65**, 837-842.

Hartman, O. (1944). Polychaetous annelids, Part VI. Paraonidae, Magelonidae, Ctenodrilidae and Sabellariidae. In *Allan Hancock Pacific Expeditions*. Vol. 10, pp. 311-389. Los Angeles: University of California Publications.

Jensen, R. A. and Morse, D. E. (1988). The bioadhesive of *Phragmatopoma californica* tubes - a silk-like cement containing L-Dopa. *J. Comp. Physiol. B Biochem. Syst. Environ. Physiol.* **158**, 317-324.

Kellermayer, M. S. Z. and Bustamante, C. (1997). Folding-unfolding transitions in single titin molecules characterized with laser tweezers. *Science* **276**, 1112-1116.

Kröger, N., Bergsdorf, C. and Sumper, M. (1994). A new calcium-binding glycoprotein family constitutes a major diatom cell-wall component. *EMBO J.* **13**, 4676-4683.

Labeit, D., Watanabe, K., Witt, C., Fujita, H., Wu, Y. M., Lahmers, S., Funck, T., Labeit, S. and Granzier, H. (2003). Calcium-dependent molecular spring elements in the giant protein titin. *Proc. Natl. Acad. Sci. USA* **100**, 13716-13721.

Leckband, D. and Sivasankar, S. (2000). Mechanism of hemophilic cadherin adhesion. *Curr. Opin. Cell Biol.* **12**, 587-592.

Lee, H., Scherer, N. F. and Messersmith, P. B. (2006). Single molecule mechanics of mussel adhesion. *Proc. Natl. Acad. Sci. USA* **103**, 12999-13003.

Nagar, B., Overduin, M., Ikura, M. and Rini, J. M. (1996). Structural basis of calcium-induced E-cadherin rigidification and dimerization. *Nature* **380**, 360-364.

Neihof, R. A. and Loeb, G. I. (1972). The surface charge of particulate matter in seawater. *J. Limnol. Oceanogr.* **17**, 7-16.

Prakasam, A., Chien, Y. H., Maruthamuthu, V. and Leckband, D. E. (2006). Calcium site mutations in cadherin: impact on adhesion and evidence of cooperativity. *Biochemistry* **45**, 6930-6939.

Rief, M., Gautel, M., Oesterhelt, F., Fernandez, J. M. and Gaub, H. E. (1997). Reversible unfolding of individual titin immunoglobulin domains by AFM. *Science* **276**, 1109-1112.

Simmons, S. A., Zimmer, R. K. and Zimmer, C. A. (2005). Life in the lee: local distributions and orientations of honeycomb worms along the California coast. *J. Mar. Res.* **63**, 623-643.

Stewart, R. J., Weaver, J. C., Morse, D. E. and Waite, J. H. (2004). The tube cement of *Phragmatopoma californica*: a solid foam. *J. Exp. Biol.* **207**, 4727-4734.

Vovelle, J. (1965). Le tube de *Sabellaria alveolata* (L.) Annelide polychete hermellidae et son ciment etude ecologique, experimentale, histologique et histochimique. *Arch. Zool. Exp. Gen.* **106**, 1-180.

Wainwright, S. A., Biggs, W. D., Currey, J. D. and Gosline, J. M. (1982). *Mechanical Design in Organisms*. Princeton: Princeton University Press.

Waite, J. H., Jensen, R. A. and Morse, D. E. (1992). Cement precursor proteins of the reef-building polychaete *Phragmatopoma californica* (Fewkes). *Biochemistry* **31**, 5733-5738.

Waite, J. H., Andersen, N. H., Jewhurst, S. and Sun, C. J. (2005). Mussel adhesion: finding the tricks worth mimicking. *J. Adhes.* **81**, 297-317.

Young, G. A. and Crisp, D. J. (1982). Marine animals and adhesion. In *Adhesion 6* (ed. K. W. Allen), pp. 19-39. Barking: Applied Science.

Zhao, H., Sun, C. J., Stewart, R. J. and Waite, J. H. (2005). Cement proteins of the tube-building polychaete *Phragmatopoma californica*. *J. Biol. Chem.* **280**, 42938-42944.